Pelizaeus-Merzbacher-like Disease Caused by AIMP1/p43 Homozygous Mutation

Miora Feinstein,[1] Barak Markus,[1] Iris Noyman,[2] Hannah Shalev,[2] Hagit Flusser,[2] Ilan Shelef,[3] Keren Liani-Leibson,[1] Zamir Shorer,[2] Idan Cohen,[1] Shareef Khateeb,[1] Sara Sivan,[1] and Ohad S. Birk[1,4,*]

Pelizaeus-Merzbacher disease is an X-linked hypomyelinating leukodystrophy caused by *PLP1* mutations. A similar autosomal-recessive phenotype, Pelizaeus-Merzbacher-like disease (PMLD), has been shown to be caused by homozygous mutations in *GJC2* or *HSPD1*. We report a consanguineous Israeli Bedouin kindred with clinical and radiological findings compatible with PMLD in which linkage to *PLP1*, *GJC2*, and *HSPD1* was excluded. Through genome-wide homozygosity mapping and mutation analysis, we demonstrated in all affected individuals a homozygous frameshift mutation that fully abrogates the main active domain of *AIMP1*, encoding ARS-interacting multifunctional protein 1. The mutation fully segregates with the disease-associated phenotype and was not found in 250 Bedouin controls. Our findings are in line with the previously demonstrated inability of mutant mice lacking the *AIMP1/p43* ortholog to maintain axon integrity in the central and peripheral neural system.

The prototype of early-onset hypomyelinating leukodystrophies is X-linked Pelizaeus-Merzbacher disease (PMD [MIM 312080]), caused by mutations in *PLP1* (MIM 300401) encoding proteolipid protein lipophilin, which is the predominant myelin protein present in the central nervous system (CNS).[1] Pelizaeus-Merzbacher-like disease (PMLD [MIM 608804, 612233]) is clinically and neuroradiologically similar to classical PMD but is not associated with PLP1 mutations.[2] Autosomal-recessive PMLD was shown to be caused by recessive heterogeneous mutations in *GJC2* (MIM 608803) encoding one of the Gap-junction-protein family of homologous connexins. *GJC2* is expressed specifically in oligodendrocytes, and its expression is regulated in parallel with other myelin genes.[3,4] Other cases of recessive PMLD were demonstrated to be due to mutations in *HSPD1* (MIM 118190). *HSPD1* is a member of the heat shock protein (HSP) family, proteins that are highly conserved throughout evolution and that play a crucial role in cell maintenance and survival. The protein encoded by *HSPD1*, also known as mitochondrial Hsp60 chaperonin, is a major component of the protein-folding system inside the mitochondrial matrix. Hsp60, together with its cochaperonin Hsp10, produces large and efficient protein-editing machinery that facilitates proper folding and assembly of mitochondrial-imported proteins and corrects misfolded polypeptides generated under mitochondrial oxidative stress.[2] In the past few years, further cases of PMLD have been demonstrated in which no *GJC2* or *HSPD1* mutations were found, implying the presence of yet-undiscovered PMLD loci and/or genes.[2]

Six individuals of three related families of consanguineous Israeli Bedouin kindred, as well as a single individual of another very remotely related consanguineous family of the same tribe, presented with apparently autosomal-recessive PMLD (Figure 1). The medical records of all seven affected individuals were reviewed, and four of the surviving five individuals underwent careful clinical evaluation by a pediatric neurologist and a clinical geneticist, followed by thorough biochemical laboratory testing and MRI. The study was approved by the Institutional Review Board of Soroka Medical Center, and informed consent was obtained from all participants or their legal guardians. In all four affected individuals that were studied in depth (with similar findings in the records of the three other patients), the disease phenotype was of severe rapid neurological deterioration progressing over the first months of life. As seen in Table 1, all affected individuals had severe failure to thrive (weight 3.5–4.5 standard deviation [SD] below average), with a concordant head circumference 2.5–4 SD below average. All had severe global developmental delay/mental retardation with lack of speech, as well as axial hypotonia. Progressive spastic paraparesis appeared within the first year, with wasting of lower limbs and positive pyramidal signs. Progressive joint contractures and kyphoscoliosis were evident as early as 2–3 years of age. Fast horizontal or rotary nystagmus, evident at age 2–3 months, was the presenting sign in most patients. All had coarse faces, most had slow pupillary reflexes, and two of the patients had seizures. Abnormal EEG patterns were noted: patient III-25, tested at age 9 months, had slow background with numerous slow generalized and bilateral spike activity. Patient IV-3, tested at 2 and 4.5 years, had generalized epileptiform activity. Patients II-1 (kindred 2), IV-3, and III-25 (Figure 1) underwent intensive laboratory work: complete blood count, routine blood chemistry, creatine-phosphokinase, cholesterol and triglycerids, ammonia, thyroid function tests, blood pH, lactate, pyruvate, blood amino acids, carnitine, acylcarnitine, very long chain fatty acids, and biotinidase were normal in all patients, as were urine tests for

[1]The Morris Kahn Laboratory of Human Genetics at the National Institute of Biotechnology in the Negev, Beer Sheva 84101, Israel; [2]Division of Pediatrics, Ben-Gurion University of the Negev, Beer Sheva 84101, Israel; [3]Diagnostic Imaging Institute, Ben-Gurion University of the Negev, Beer Sheva 84101, Israel; [4]Genetics Institute at Soroka Medical Center, Ben-Gurion University of the Negev, Beer Sheva 84101, Israel
*Correspondence: obirk@bgu.ac.il
DOI 10.1016/j.ajhg.2010.10.016.

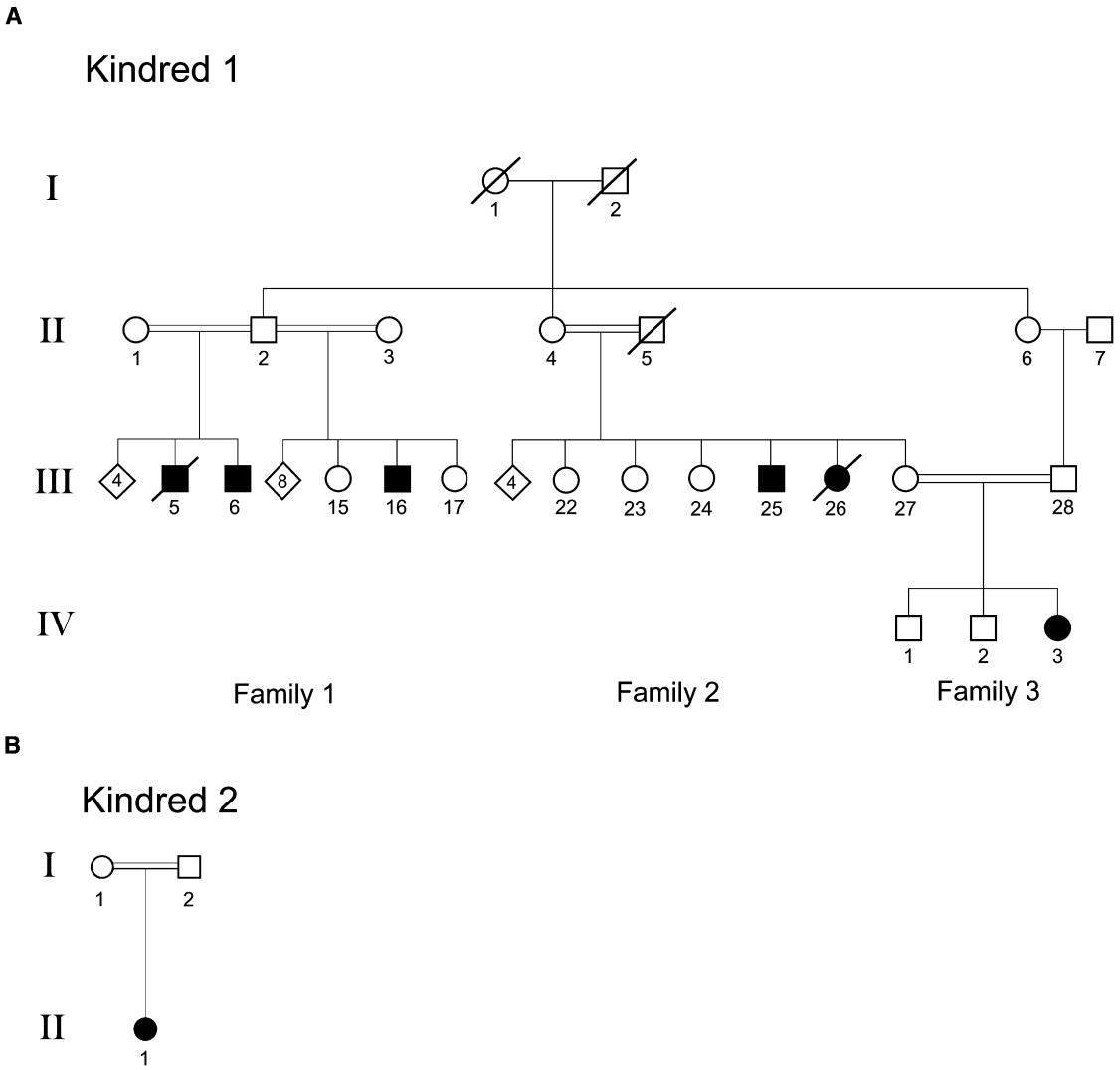

Figure 1. Pedigree of the Affected Israeli Bedouin Kindred
(A and B) The pedigree is compatible with autosomal-recessive heredity. (A) and (B) are branches of a single extended tribe, remotely related (not first or second degree).

mucopolysaccharides and oligosaccharides and cerebrospinal fluid tests for glucose, protein, and cells. Vanillylmandelic acid was in normal range for patient II-1. Enzymatic assays ruled out metachromatic leukodystrophy (MIM 250100) and Krabbe disease (MIM 245200) for patients III-25 and II-1, as well as Gangliosidosis type 1 and 2 (MIM 230500, 230600) and neuronal ceroid lipofuscinosis types 1 and 2 (MIM 256730, 204500) for patient II-1. Rectal biopsy for patient III-25 demonstrated no evidence of a storage disease.

MRI findings were very similar in all affected individuals, showing arrest of myelination. The T2-weighted images showed high signal of hypomyelination starting at a normal stage (Figure 2A), as well as high signal on flair (Figure 2B). These findings were seen as low signal on T1-weighted images (Figure 2D). On diffusion-weighted images, exponential apparent diffusion coefficient (eADC) showed low signal (Figure 2E), representing increased diffusivity secondary to hypomyelinated brain tissue. Magnetic resonance spectroscopy demonstrated relative decrease of N-acetylaspartate within the white matter, likely because of axonal degeneration (Figure 2C). Generalized brain atrophy, especially of the corpus callosum (Figure 2F), was noted.

DNA samples of the five surviving patients and 14 of their first-degree relatives were available for molecular analyses. With a clinical diagnosis of PMLD, and assuming a founder effect, we used microsatellite markers (as previously described)[5] to test the affected individuals for homozygosity at the loci of *GJC2* and *HSPD1*, whose mutations are known to cause PMLD. In short, genomic DNA was extracted from peripheral lymphocytes, and microsatellite markers were derived from Marshfield maps.[6] Intronic primer pairs were designed with the Primer3 (version 0.4.0) software, based on DNA sequences obtained from UCSC Genome Browser (sequences available on request).

Table 1. Clinical Signs and Symptoms

Clinical Sign/Symptom	Patient III-16	Patient III-25	Patient IV-3	Patient II-1, Kindred 2	Patient III-6	Patient III-5	Patient III-26
Present age	19 yrs.	15 yrs.	5 yrs.	16 mos.	26 yrs.	Died 13 yrs.	Died 24 yrs.
Weight (percentile)	−4.5 SD	−4.5 SD	−3.5 SD	−3.5 SD	FTT	FTT	FTT
Head circumference (percentile)	−4 SD	−4 SD	−4 SD	−2.5 SD	ND	ND	ND
Global developmental delay/mental retardation	Severe	Severe	Severe	Severe	Severe	Severe	Severe
Seizures	−	+	+	−	−	ND	ND
Mild dysmorphism	+	+	+	+	+	+	+
Sight	Impaired	Impaired	Impaired	Impaired	Impaired	Impaired	Impaired
Speech	−	−	−	−	−	−	−
Nystagmus: age of onset (mos.)	2	1.5	3	2	2–3	2–3	2–3
Exotropia	−	−	+	+	ND	ND	ND
Slow pupillary reflex	+	+	+	-	ND	ND	ND
Pale fundi	+	+	-	-	ND	ND	ND
Axial hypotonia	+	+	+	+	+	+	+
Limb spasticity/spastic paraparesis	+	+	+	+	+	+	+
Pyramidal signs	+	+	+	+	ND	ND	ND
Wasting of lower limbs	+	+	+	−	+	+	+
Kyphoscoliosis	+	+	+	−	+	+	+
Joint contractures	+	+	+	−	+	+	+

The following abbreviations are used: FTT, failure to thrive, no precise measurements available; ND, no data available.

Polymerase chain reaction (PCR) products were separated on polyacrylamide gel with silver staining for detection as previously described.[6] Affected individuals did not share homozygosity at any of the two loci (data not shown).

Next, we did genome-wide linkage analysis with Affymetrix GeneChip Human Mapping 500K Set Nsp microarrays, testing five affected individuals (subjects III-6, III-16, III-25, and IV-3 of kindred 1 and subject II-1 of kindred 2) and seven of their first-degree relatives, according to the Affymetrix GeneChip Mapping Assay protocol as previously described.[6] Homozygosity by descent analysis was carried out with an in-house-generated tool for homozygosity mapping (B.M. and O.S.B., unpublished data). The analysis identified a 9.52 Mb segment of homozygosity on chromosome 4q23-q25 that was common to all five patients. Few additional significantly smaller regions of shared homozygosity shorter than 1 Mb were spotted. However, because none of these were contained within larger stretches of individual homozygosity, we first analyzed the 4q23-q25 locus. Fine mapping of this locus was performed on samples of the five samples of affected individuals included in the study and their close relatives by genotyping with additional microsatellite markers derived from Marshfield maps or with novel markers designed based on Tandem Repeats Finder (TRF) program and the UCSC Human Genome Database. Analysis with polymorphic markers chr4:98663671-98663717, D4S1647, and D4S1564 narrowed down the 4q23-q25 region to 8.94 Mb spanning 867 consecutive SNPs between markers rs10026181and rs203202 at physical positions 98814118 and 108329618, respectively. Genotyping with eight additional microsatellite markers within the homozygosity interval in five affected children and their close relatives (Figure 3) further substantiated the identification of the chromosome 4q23-q25 interval as the disease-associated locus. Multipoint LOD score calculation with SUPERLINK[7] was done for markers D4S1647, D4S2634, D4S421, D4S1591, chr4:103271298-103271353, chr4:104134017-104134065, D4S2913, chr4:106364749-106364794, and chr4:107336226-107336269 on 4q24 (kindred 1, Figure 1). The calculations were done assuming an autosomal-recessive mode of inheritance with penetrance of 0.99, a disease mutant gene frequency of 0.01, and a uniform distribution of allele frequencies. The maximum multipoint LOD score calculated for kindred 1 was 4.25. All affected individuals in both kindreds 1 and 2 shared a common homozygous haplotype between markers D4S2634 and chr4:107336226-107336269, supporting a common ancestral origin for this locus.

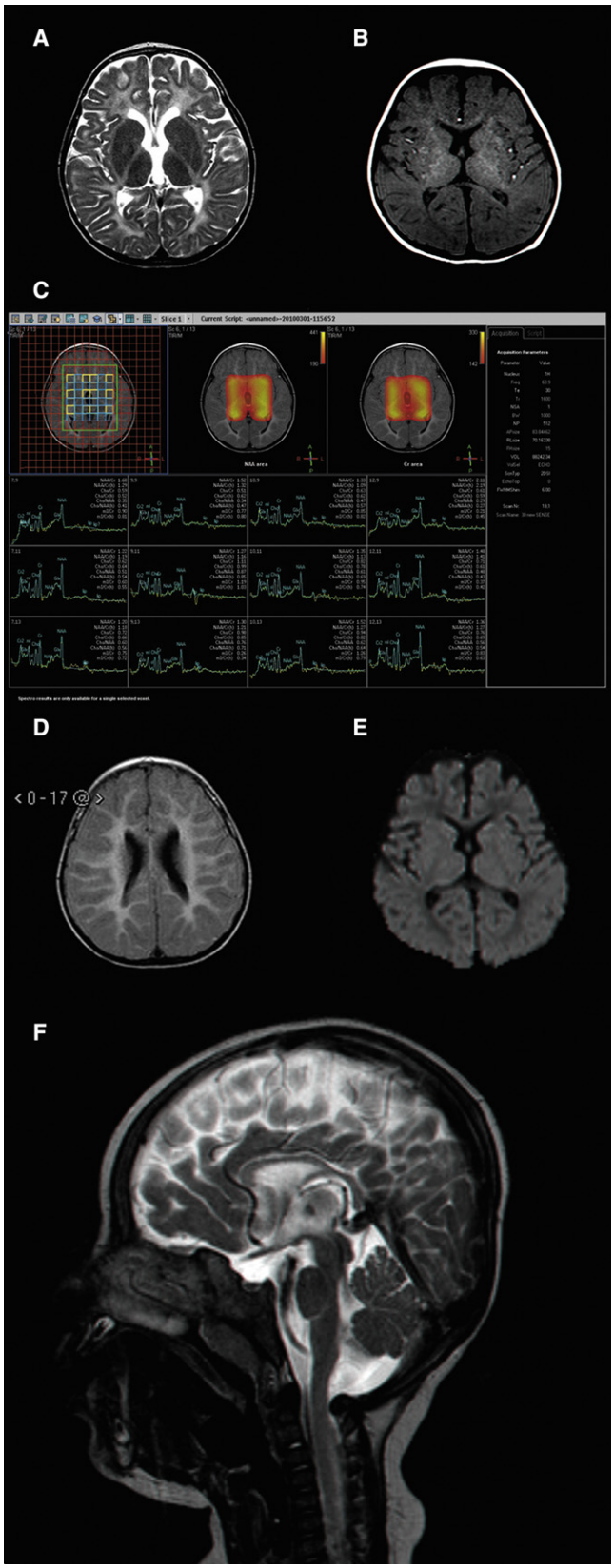

Figure 2. MRI of Two Affected Individuals
(A–C) Girl age 5 years with severe form of PMLD. The images demonstrate arrested myelination and reduced N-acetylaspartate. The T2-weighted images showed high signal of hypomyelination starting at a normal stage (A), as well as high signal on flair (B). Magnetic resonance spectroscopy demonstrated relative decrease of N-acetylaspartate within the white matter, likely because of axonal degeneration (C).
(D–F) Girl age 14 months with severe form of PMLD. The images demonstrate incomplete myelination and corpus callosum atrophy. These findings were seen as low signal on T1-weighted images (D). On diffusion-weighted images, eADC showed low signal (E) representing increased diffusivity secondary to hypomyelinated brain tissue. Generalized brain atrophy, especially of the corpus callosum, was noted (F).

We next proceeded to prioritize and sequence candidate genes within the identified locus. The clinical presentation of the patients of both kindred was determined to be similar to PMLD. Thus, to obtain a prioritized list of the 39 candidate genes within the locus, we used our Syndrome to Gene (S2G) software,[8] inserting *GJC2* (whose mutations are known to cause PMLD) as a reference gene. Because we find sequencing of lymphoblastoid cDNA more efficient than sequencing genomic DNA (when possible), we did Epstein Barr virus (EBV) transformation of lymphocytes of affected individuals as previously described.[9] RNA was extracted from cultured cells of EBV-transformed lymphoblastoid cell lines with the RNeasy Mini Kit (QIAGEN), and cDNA was reverse transcribed by the Verso RT-PCR kits (TAMAR) according to the manufacturer's protocol.[10] Primer pairs for PCR amplification from cDNA and/or exons of genomic DNA (including flanking intron sequences) of the 39 genes in the putative 4q24 locus were designed based on the known mRNA and genomic sequences with Primer3. Primer sequences and PCR conditions are available upon request. PCR products were directly sequenced with ABI PRISM 3730 DNA Analyzer according to the protocols of the manufacturer (Applied Biosystems). Sequence variations (Table 2) were confirmed by bidirectional sequencing. Sequencing of the entire coding region and intron-exon borders of the top 15% of the genes on the prioritized list identified a single frameshift mutation common to all affected individuals: a c.292_293delCA (p.Gln98ValfsX30) mutation in exon 4 of AIMP1/p43, position 292–293 in the UCSC Consensus Coding Sequence, variant NM_001142415.1 (Figure 4). The mutation is predicted to truncate the major conserved functional domains of AIMP1 (Figure 4). Testing for the *AIMP1* mutation in the entire family and controls was done via restriction analysis, based on the fact that the mutation abrogates an HpyCH4III restriction site. Because there is another HpyCH4III recognition site only 17 bp apart (that is common to both wild-type and mutated sequences, based on New England Biolabs NEBcutter), PCR primer pairs were designed in which the reverse primer included part of that second HpyCH4III site, introducing a single nucleotide change (A314T) that eliminates this second HpyCH4III restriction site. PCR amplification of genomic DNA with this primer set gave a 198 bp fragment, generating HpyCH4III (TaaI-Fermentas) differential cleavage products of the mutant (uncut, 198 bp) versus wild-type alleles (158 bp and 40 bp). Fragments were

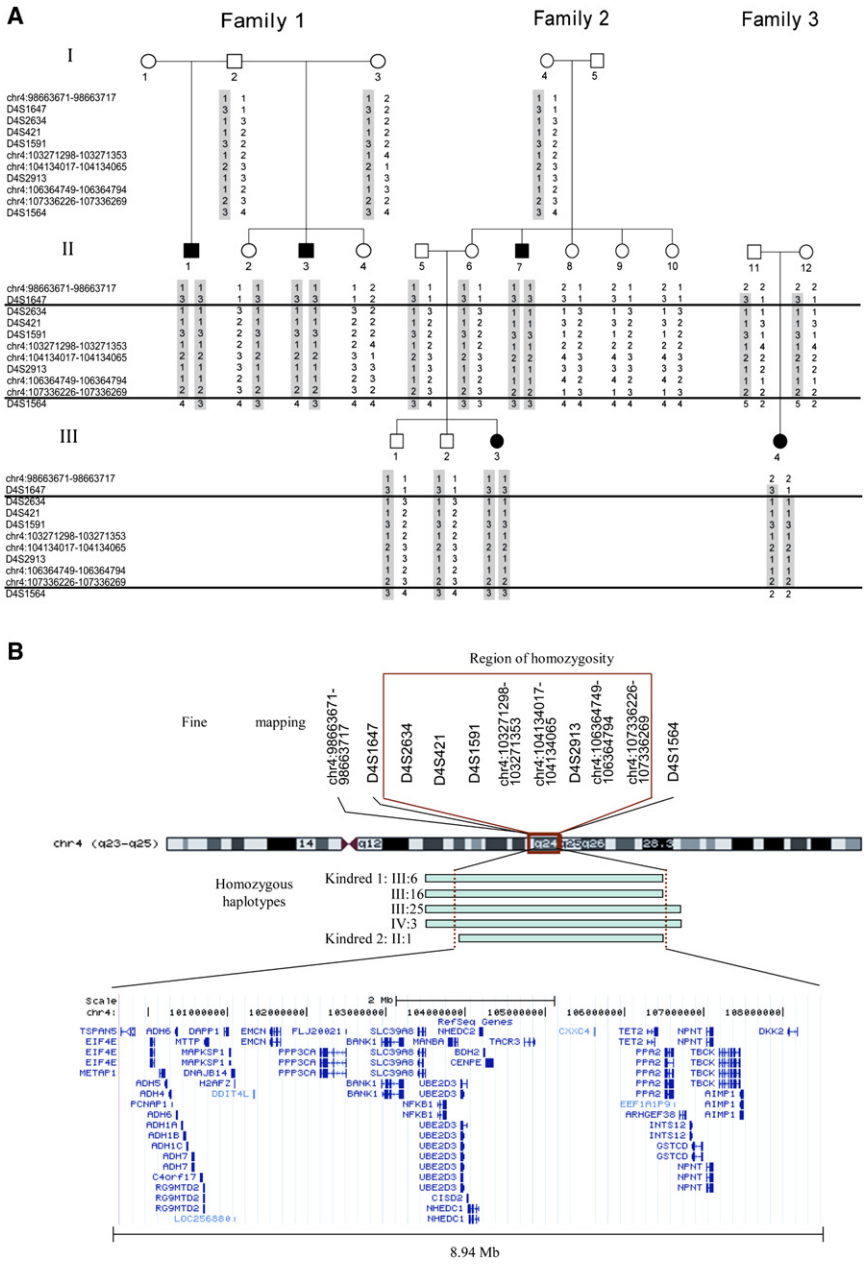

Figure 3. Fine Mapping of the 4q24 Locus in Kindred 1 and Kindred 2

(A) Disease-associated haplotype shown in boxes. Markers D4S2634 and chr4:107336226-107336269 define the minimal homozygosity locus associated with the disease. Blank spaces indicate nongenotyped markers.

(B) Schematic presentation of the defined locus and the genes it contains (UCSC). Markers within the homozygosity locus are boxed.

separated by electrophoresis on 3% agarose gel. PCR amplification primers were F-5′-AGAGTTCCCATTTGTGG TTCA-3′ and R-3′-TTCTTTGGTACCAGAAGATTCGG-5′.

Using this restriction analysis, we showed complete segregation (and thus full penetrance) of the mutation with the disease-associated phenotype in all investigated family members, heterozygosity in all obligatory carrier parents, and no homozygosity in nonaffected individuals. The mutation was not present in 500 chromosomes of healthy ethnically matched control samples. Sequencing the entire coding region and intron-exon borders of 13 other genes and partial sequences of 12 additional genes within the 4q23-q25 locus (some of which were not predicted by S2G) identified no further mutations in those individuals (data not shown).

We have thus showed through homozygosity mapping,[11,12] followed by mutation analysis of candidate genes within the 4q24 locus, a homozygous frameshift mutation in *AIMP1/p43* as the cause of an autosomal-recessive hypomyelinating leukodystrophy with the characteristics of PMLD. Prioritizing of candidate genes within the defined locus was done with S2G.[8] The software selects a prioritized list of candidate genes for any syndrome, based on their known molecular interactions with genes associated with phenotypically similar syndromes. It is of interest to note that *AIMP1* was in the top 15% of the S2G prioritized list of 39 genes within the 4q23-q25 locus, demonstrating the effectiveness of our S2G software in the identification of disease genes.

AIMP1 has three splice variants (RefSeq NM_001142415.1, NM_001142416.1, NM_004757.3), two of which encode the same 312 aa protein product. The deletion leads to a frameshift mutation, p.Gln98ValfsX30, disrupting the original protein sequence after 97 aa, causing the early appearance of a stop codon at position 127 in two splice variants. The third splice variant (NM_001142416.1) contains a c.364_365delCA mutation that leads to a mutant protein sequence (p.Gln122ValfsX30). The deleted part in the mutant protein contains the most important AIMP1/p43 predicted domains (derived from SMART[13]) that are highly conserved across AIMP1/p43 homologs from seven different nonhuman species (Figure 3E). The truncated protein lacks the tRNA-binding domain (aa 151–252), a domain needed for interaction with HSP90B1 (aa 54–195), and a segment required for induction of inflammation (aa 147–312), as well as regions that control angiogenesis by a biphasic mechanism, manipulating tube formation and endothelial cell death

Table 2. Gene Variants Found in Sequencing of DNA Sample of Affected Individual

Gene	SNP
MANBA	rs227368
DDIT4L	rs58706659, rs56763427
CENPE	rs61751592
NPNT	rs4340795

(aa 114–192 and aa 101–114), respectively. All domain locations refer to variants NP_001135887 and NP_004748 (Figures 3D and 3E).[14]

AIMP1 (initially termed P43) is known to undergo cleavage by caspase 7 in response to apoptosis to produce endothelial monocyte-activating polypeptide II (EMAP-II), which is involved in the control of angiogenesis, inflammation, and wound healing.[14] The release of this cytokine renders the tumor-associated vasculature sensitive to tumor necrosis factor.[15] The part of the AIMP1 protein that is essential for these functions (that is missing in the mutated protein, Figure 4) is extremely conserved throughout evolution. Interestingly, the affected individuals did not present with any clinically significant immune deficiency. It is plausible that the failure of the patients to thrive might be due in part to disturbances in angiogenesis. However, further studies are required to discern possible subtle effects of the AIMP1 mutation on angiogenesis and inflammation in the affected individuals of this kindred.

The neurological phenotype seen in the patients is not surprising. There is ample evidence of a major role of

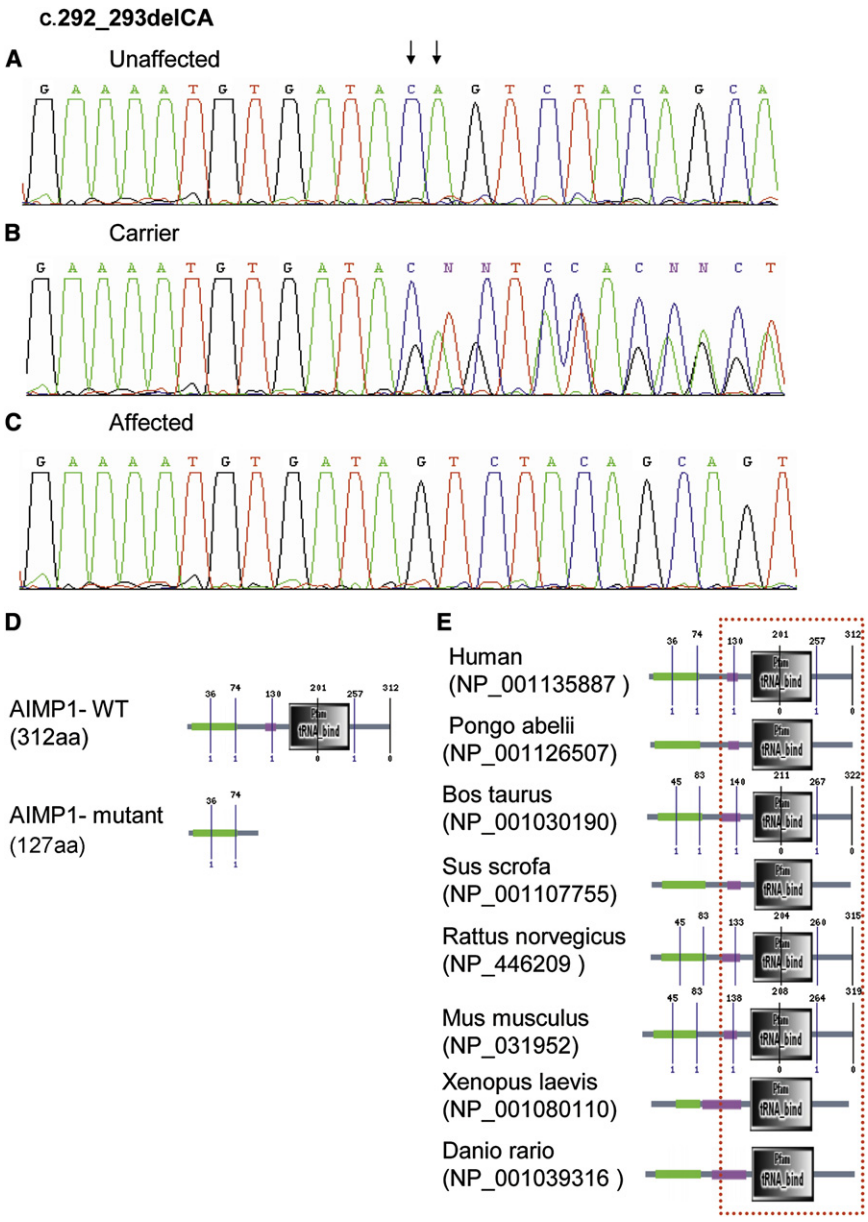

Figure 4. The c.292_293delCA Mutation in Exon 4 of *AIMP1*

(A–C) Sequence analysis is shown for an unaffected individual (A), an obligatory carrier (B), and an affected individual (C).

(D) *SMART* display of human AIMP1 domains along the wild-type sequence versus the mutant protein. The aberrant region in the mutant protein includes the tRNA-binding domain, a sequence needed for interaction with *HSP90B1*, and a region required for endothelial cell death and migration.[13] The protein sequence is altered after 97 aa, and a stop codon truncates the protein after 127 aa.

(E) Conservation of AIMP1 domains throughout evolution. Deleted area is boxed.

AIMP1 in neurons: the AIMP1/p43 mouse ortholog has been shown to be expressed in neurons of the CNS and the spinal cord in mice and to be associated directly with NF-L (light chain of the neurofilaments), modulating their phosphorylation and assembly in the neuronal network. NF-L is the pivotal subunit of NFs, the major intermediate filament (IF) of neurons and axons, and it plays a crucial role in the maintenance of the neural cytoskeleton in the CNS.[16–20] Depletion of the AIMP1/p43 protein causes hyperphosphorylation of NF proteins and NF network disassembly in primary cultured neurons and motor axons, resulting in phenotypes similar to those observed in mice lacking the mouse ortholog of *NEFL* (MIM 162280, encoding NF-L). The hyperphosphorylation of NFs in mutant mice lacking the functional AIMP1/p43 mouse ortholog could result from activation of certain kinases that are otherwise suppressed by AIMP1/p43 under physiological conditions.[21–24] Thus, AIMP1/P43 functions in a fundamental role of regulating NF-L and maintains CNS-cytoskeleton integrity. Because of its interaction with NF-L, and because of NF-L's association to Charcot-Marie-Tooth (CMT) neuropathies, AIMP1 has also been suggested to be a potential molecular linker between components of the protein biosynthesis machinery (ARSs) and NFs in CMT neuropathy, on the basis of similarity between clinical features of the disease and those of AIMP1 null mice.[15,20] Because AIMP1 is classified as a fundamental regulator of NF-L and thus a regulator of axon development and maintenance,[20] its molecular interactions with NF-L are likely associated with the disease mechanism in the kindred studied.

Mutations in *NEFL* cause autosomal-dominant neuropathies that are classified either as axonal CMT type 2 (CMT2 [MIM 607648]) or demyelinating CMT type 1 (CMT1 [MIM 607734]) diseases. CMT patients have motor and sensory neuropathies characterized by progressive muscular atrophy and sensory loss in the distal limbs.[17] CMT1 usually results from myelin alteration, and histological examination of CMT1 neurons often reveals extensive segmental demyelination and remyelination.[18] CMT1 patients studied over the last decade presented diverse phenotypes, including mental retardation, pyramidal signs, and cerebellar atrophy.[19] It has been suggested that mutant NF-L subunits cause neurological disease through altering the formation and maintenance of the cytoskeletal network,[16] and studies have shown the connection of NF-L to neurodegenerative diseases.

AIMP1 also functions as a noncatalytic component of the multisynthetase complex. This complex is comprised of a bifunctional glutamyl-prolyl-tRNA synthetase, the monospecific isoleucyl, leucyl, glutaminyl, methionyl, lysyl, arginyl, and aspartyl tRNA synthetases, and three auxiliary proteins, EEF1E1/p18, AIMP2/p38, and AIMP1/p43, together catalyzing the ligation of amino acids to their cognate tRNAs.[25] Although tRNA formation and processing are obviously essential in all tissues of the human body, disturbances in such processes have been shown to lead to human phenotypes that affect mostly the nervous system. Pontocerebellar hypoplasia (PCH) is a heterogeneous group of disorders characterized by an abnormally small cerebellum and brainstem. PCH type 2, characterized by progressive microcephaly combined with extrapyramidal dyskinesia and chorea, epilepsy, and normal spinal cord findings, is caused by mutations in genes involved in tRNA processing: TSEN54, TSEN2, and TSEN34, which are subunits of the tRNA splicing endonuclease complex.[26] Furthermore, we have recently demonstrated that a homozygous mutation in *SepSecS* (which normally catalyzes the conversion of Sep-tRNA to Sec-tRNA) abrogates the formation of the 21st amino acid selenocyetsine (the only genetically encoded amino acid in humans whose biosynthesis occurs on its cognate tRNA), leading to a neurodegenerative phenotype of progressive cerebrocerebellar atrophy presenting with nondysmorphic profound mental retardation, progressive microcephaly, and severe spasticity with myoclonic or generalized tonic-clonic seizures.[27] Thus, it is not surprising that a mutation in a molecule essential for tRNA formation or processing leads to a neurospecific human phenotype.

Further support of the *AIMP1* mutation being the underlying cause of the PMLD phenotype comes from the phenotype of mutant mice lacking the functional AIMP1/P43 ortholog:[20] mice lacking the AIMP1/p43 ortholog in their central nervous system displayed weight loss and spontaneous spastic tremors, could not extend their hind limbs when suspended by the tail, and exhibited slower gaits and decreased motor activity. Histological studies showed widespread muscle atrophy with pronounced atrophy of the large gastrocnemius muscle of the hind limb (much like that shown in the patients), including the reduction of muscle fiber density, muscle atrophy, fibrosis, and clustering of muscle fibers.[20]

In conclusion, we have identified a homozygous deletion mutation in *AIMP1/p43* as the cause of a severe neurodegenerative disorder whose phenotype is commensurate with the diagnosis of PMLD with coarse face as a unique feature. Our findings allow carrier testing and early prenatal diagnosis in a large consanguineous population in southern Israel and hopefully in other PMLD families worldwide. The molecular mechanisms underlying the phenotype are likely associated with the role of AIMP1 in NF-L phosphorylation, affecting maintenance of the neural cytoskeleton in the CNS. The phenotype might arise in part also from abrogation of the function of AIMP1 in a complex catalyzing the ligation of amino acids to their cognate tRNAs. Molecular cascades possibly tying together AIMP1 with PLP1, GJC2, or HSPD1, whose mutations cause similar phenotypes, are yet to be elucidated.

Acknowledgments

The authors deeply thank the Israel Science Foundation, the Morasha Legacy Heritage Fund, and the Morris Kahn Family Foundation for making this study possible.

Received: August 22, 2010
Revised: October 10, 2010
Accepted: October 14, 2010
Published online: November 18, 2010

Web Resources

The URLs for data presented herein are as follows:

Chromas, http://www.technelysium.com.au/chromas.html
HaploPainter, http://haplopainter.sourceforge.net/index.html
Marshfield Maps, http://research.marshfieldclinic.org/genetics/GeneticResearch/compMaps.asp
New England Biolabs NEBcutter version 2.0, http://tools.neb.com/NEBcutter2/
Online Mendelian Inheritance in Man (OMIM), http://www.ncbi.nlm.nih.gov/Omim/
Primer3 (v. 0.4.0): Pick primers from a DNA sequence, http://frodo.wi.mit.edu/primer3/
Simple Modular Architecture Research Tool (SMART), http://smart.embl-heidelberg.de/
Superlink online version 1.5, http://bioinfo.cs.technion.ac.il/superlink-online/
Syndrome to Gene (S2G), http://fohs.bgu.ac.il/s2g
UCSC Genome Browser, http://genome.ucsc.edu/

References

1. van der Knaap, M.S., Breiter, S.N., Naidu, S., Hart, A.A., and Valk, J. (1999). Defining and categorizing leukoencephalopathies of unknown origin: MR imaging approach. Radiology *213*, 121–133.
2. Magen, D., Georgopoulos, C., Bross, P., Ang, D., Segev, Y., Goldsher, D., Nemirovski, A., Shahar, E., Ravid, S., Luder, A., et al. (2008). Mitochondrial hsp60 chaperonopathy causes an autosomal-recessive neurodegenerative disorder linked to brain hypomyelination and leukodystrophy. Am. J. Hum. Genet. *83*, 30–42.
3. Uhlenberg, B., Schuelke, M., Rüschendorf, F., Ruf, N., Kaindl, A.M., Henneke, M., Thiele, H., Stoltenburg-Didinger, G., Aksu, F., Topaloğlu, H., et al. (2004). Mutations in the gene encoding gap junction protein alpha 12 (connexin 46.6) cause Pelizaeus-Merzbacher-like disease. Am. J. Hum. Genet. *75*, 251–260.
4. Salviati, L., Trevisson, E., Baldoin, M.C., Toldo, I., Sartori, S., Calderone, M., Tenconi, R., and Laverda, A. (2007). A novel deletion in the GJA12 gene causes Pelizaeus-Merzbacher-like disease. Neurogenetics *8*, 57–60.
5. Birnbaum, R.Y., Zvulunov, A., Hallel-Halevy, D., Cagnano, E., Finer, G., Ofir, R., Geiger, D., Silberstein, E., Feferman, Y., and Birk, O.S. (2006). Seborrhea-like dermatitis with psoriasiform elements caused by a mutation in ZNF750, encoding a putative C2H2 zinc finger protein. Nat. Genet. *38*, 749–751.
6. Khateeb, S., Flusser, H., Ofir, R., Shelef, I., Narkis, G., Vardi, G., Shorer, Z., Levy, R., Galil, A., Elbedour, K., and Birk, O.S. (2006). PLA2G6 mutation underlies infantile neuroaxonal dystrophy. Am. J. Hum. Genet. *79*, 942–948.
7. Silberstein, M., Tzemach, A., Dovgolevsky, N., Fishelson, M., Schuster, A., and Geiger, D. (2006). Online system for faster multipoint linkage analysis via parallel execution on thousands of personal computers. Am. J. Hum. Genet. *78*, 922–935.
8. Gefen, A., Cohen, R., and Birk, O.S. (2010). Syndrome to gene (S2G): In-silico identification of candidate genes for human diseases. Hum. Mutat. *31*, 229–236.
9. Narkis, G., Ofir, R., Manor, E., Landau, D., Elbedour, K., and Birk, O.S. (2007b). Lethal congenital contractural syndrome type 2 (LCCS2) is caused by a mutation in ERBB3 (Her3), a modulator of the phosphatidylinositol-3-kinase/Akt pathway. Am. J. Hum. Genet. *81*, 589–595.
10. Narkis, G., Ofir, R., Landau, D., Manor, E., Volokita, M., Hershkowitz, R., Elbedour, K., and Birk, O.S. (2007a). Lethal contractural syndrome type 3 (LCCS3) is caused by a mutation in PIP5K1C, which encodes PIPKI gamma of the phophatidylinsitol pathway. Am. J. Hum. Genet. *81*, 530–539.
11. Botstein, D., White, R.L., Skolnick, M., and Davis, R.W. (1980). Construction of a genetic linkage map in man using restriction fragment length polymorphisms. Am. J. Hum. Genet. *32*, 314–331.
12. Lathrop, G.M., and Lalouel, J.M. (1984). Easy calculations of lod scores and genetic risks on small computers. Am. J. Hum. Genet. *36*, 460–465.
13. Schultz, J., Milpetz, F., Bork, P., and Ponting, C.P. (1998). SMART, a simple modular architecture research tool: Identification of signaling domains. Proc. Natl. Acad. Sci. USA *95*, 5857–5864.
14. Han, J.M., Park, S.G., Lee, Y., and Kim, S. (2006). Structural separation of different extracellular activities in aminoacyl-tRNA synthetase-interacting multi-functional protein, p43/AIMP1. Biochem. Biophys. Res. Commun. *342*, 113–118.
15. Kao, J., Houck, K., Fan, Y., Haehnel, I., Libutti, S.K., Kayton, M.L., Grikscheit, T., Chabot, J., Nowygrod, R., Greenberg, S., et al. (1994). Characterization of a novel tumor-derived cytokine. Endothelial-monocyte activating polypeptide II. J. Biol. Chem. *269*, 25106–25119.
16. Fabrizi, G.M., Cavallaro, T., Angiari, C., Cabrini, I., Taioli, F., Malerba, G., Bertolasi, L., and Rizzuto, N. (2007). Charcot-Marie-Tooth disease type 2E, a disorder of the cytoskeleton. Brain *130*, 394–403.
17. Georgiou, D.M., Zidar, J., Korosec, M., Middleton, L.T., Kyriakides, T., and Christodoulou, K. (2002). A novel NF-L mutation Pro22Ser is associated with CMT2 in a large Slovenian family. Neurogenetics *4*, 93–96.
18. Mersiyanova, I.V., Perepelov, A.V., Polyakov, A.V., Sitnikov, V.F., Dadali, E.L., Oparin, R.B., Petrin, A.N., and Evgrafov, O.V. (2000). A new variant of Charcot-Marie-Tooth disease type 2 is probably the result of a mutation in the neurofilament-light gene. Am. J. Hum. Genet. *67*, 37–46.
19. Abe, A., Numakura, C., Saito, K., Koide, H., Oka, N., Honma, A., Kishikawa, Y., and Hayasaka, K. (2009). Neurofilament light chain polypeptide gene mutations in Charcot-Marie-Tooth disease: Nonsense mutation probably causes a recessive phenotype. J. Hum. Genet. *54*, 94–97.
20. Zhu, X., Liu, Y., Yin, Y., Shao, A., Zhang, B., Kim, S., and Zhou, J. (2009). MSC p43 required for axonal development in motor neurons. Proc. Natl. Acad. Sci. USA *106*, 15944–15949.
21. Nixon, R.A., and Sihag, R.K. (1991). Neurofilament phosphorylation: A new look at regulation and function. Trends Neurosci. *14*, 501–506.
22. Petzold, A. (2005). Neurofilament phosphoforms: Surrogate markers for axonal injury, degeneration and loss. J. Neurol. Sci. *233*, 183–198.
23. Omary, M.B., Ku, N.O., Tao, G.Z., Toivola, D.M., and Liao, J. (2006). "Heads and tails" of intermediate filament

phosphorylation: Multiple sites and functional insights. Trends Biochem. Sci. *31*, 383–394.
24. Lee, S.W.K.G., and Kim, S. (2008). Aminoacyl-tRNA synthetase-interacting multifunctional protein 1/p43: An emerging therapeutic protein working at systems level. Expert Opin. Drug Discov. *3*, 945–957.
25. Park, S.G., Schimmel, P., and Kim, S. (2008). Aminoacyl tRNA synthetases and their connections to disease. Proc. Natl. Acad. Sci. USA *105*, 11043–11049.
26. Budde, B.S., Namavar, Y., Barth, P.G., Poll-The, B.T., Nürnberg, G., Becker, C., van Ruissen, F., Weterman, M.A., Fluiter, K., te Beek, E.T., et al. (2008). tRNA splicing endonuclease mutations cause pontocerebellar hypoplasia. Nat. Genet. *40*, 1113–1118.
27. Agamy, O., Ben Zeev, B., Lev, D., Marcus, B., Fine, D., Su, D., Narkis, G., Ofir, R., Hoffmann, C., Leshinsky-Silver, E., et al. (2010). Mutations disrupting selenocysteine formation cause progressive cerebello-cerebral atrophy. Am. J. Hum. Genet. *87*, 538–544.